Mansoura University
Faculty of Engineering
Mansoura Engineering Journal

Investigation of Film Cooling Effectiveness under Different Reynolds Numbers and Rotation Conditions

I. E. El-Helw, *S. H. El-Emam, G. I. Sultan* and W. M. El-Awady

KEYWORDS:

Film cooling, Film holes row location, Blowing ratio, Rotation, Reynolds number.

***Abstract*—The average film cooling effectiveness is numerically investigated under different conditions of Reynolds numbers and rotation speeds at the suction side of the turbine blade. Three locations of the injection holes row were checked from the blade leading edge at 10%, 31%, and 69% of the blade axial chord length. Coolant is injected from eleven cylindrical holes at rotational speeds ranged from 0 to 4600 rpm and blowing ratios ranged from 0.91 to 2. For the mainstream hot gases, the investigation is performed at five Reynolds numbers of 50,000, 87,300, 300,000, 500,000, and 700,000. The inlet temperature of the coolant is 650 K, while the hot gases inlet temperature is 1500 K for all the studied cases. Location 1 shows the optimum average film cooling effectiveness. Near the film holes, the enhancement in the average film cooling effectiveness of location 1 is by 22% than location 2 and 35% than location 3. For location 1, the effectiveness is enhanced by 57% as the blowing ratio increases from M=0.91 to M=2. For location 2, the effectiveness improves as the rotational speed increases from 0 rpm until it reaches the optimum value at 900 rpm. Also, it is perceived that as the Reynolds number increases, the effectiveness worsens because of the increase in the hot mainstream momentum.**

I. INTRODUCTION

GAS turbine manufacturers aim to maximize power output, enhance the thermal efficiency, decrease the specific fuel consumption, and reduce the engine weight [1]. Increasing turbine inlet temperature has a major impact on increasing turbine efficiency, but on the other hand, it induces several modes of failure on the blades as: thermal fatigue, creep, and erosion and corrosion [2]. The rise in the turbine inlet temperature may be achieved either by enhancing blade material which is still limited or by using cooling techniques [1]. The temperature of turbine blade can be decreased by 200°C to 300°C when 1.5% to 2% of the air mass flow rate taken from the compressor is used for cooling [1]. Various methods are used for cooling such as impingement and normal convection, but film cooling is considered as one of the most commonly used and effective methods in this approach [2]. Over the last years, film cooling is intensively investigated [3]. The main investigated parameters are the blade design configuration, shape and spacing of the film holes, and characteristics of mainstream and coolant flow.

The effect of the hot freestream Reynolds number and coolant density has been taken by Li et al. [4]. They found that

Received: (17 January, 2021) - Revised: (16 March, 2021) - Accepted: (20 March, 2021)

***Corresponding Author:** I. E. El-Helw: is with the Mechanical Power Engineering Department, Badr University Cairo, Badr 11829, Egypt (e-mail: ismail.ezz.mail@gmail.com).*

S. H. El-Emam: is with the Mechanical Power Engineering Department, Mansoura University, Mansoura 35516, Egypt (email: selemam45@yahoo.com).

G. I. Sultan: is with the Mechanical Power Engineering Department, Mansoura University, Mansoura 35516, Egypt (e-mail: gisultan@mans.edu.eg).

W. M. El-Awady: is with the Mechanical Power Engineering Department, Mansoura University, Mansoura 35516, Egypt (e-mail: Welawady@yahoo.com).

(Ser. NO. BFEMU-2101-1091)

as the hot freestream Reynolds number (Re) rises, there is an enhancement in the average film cooling effectiveness. At fixed values of (Re), the higher average blade film cooling effectiveness happens when using the higher density coolant. The influences of mainstream turbulence intensity could be found in [5-6]. They found a significant reduction of film cooling effectiveness when using a high-turbulence intensity of flow. The influence of unsteady wake has been taken by Mhetras and Han [7].

NOMENCLATURE

Symbols					
C	Blade chord length, (mm)	U	Velocity, (m/s)	μ	Dynamic viscosity, (Pa/s)
Cx	Blade axial chord length, (mm)	X	Streamwise direction, (m)	ρ	Density, (kg/m^3)
d	Hole diameter, (mm)	Y	Normal direction, (m)		
M	Blowing ratio	Z	Lateral direction, (m)	**Subscripts**	
R	Rotation speed, (rpm)	**Greek Symbols**		av	average
Re	Reynolds number	β	Primary flow angle	c	coolant
T	Temperature, (K)	η	Effectiveness	w	wall
				∞	mainstream

The effect of blowing ratio (M) was taken by Li et al. [4] and [7-8]. They predicted that as the blowing ratio (M) rises the average film cooling effectiveness get better. Also, Kwak and Han [8] found that as the blowing ratio increases the heat transfer coefficient reduces. The effect of the ratio of the coolant mass flow to the hot freestream mass flow and coolant temperature on film cooling effectiveness was performed by Garg and Gaugler [9]. They found that film cooling effectiveness reduces at higher coolant temperatures. But when the ratio of the coolant mass flow to the hot freestream mass flow was 5% or more, higher effectiveness occurs. Liu et al. [10] and Yao et al. [11] presented the effect of cylindrical and console holes on film cooling effectiveness. The cylindrical holes showed a lower film coverage area and a lower film cooling effectiveness than the console ones mainly at large values of blowing ratio. Nguyen et al. [12] found a lower film cooling effectiveness that occurs by cylindrical-shaped holes compared with conical-shaped ones for low and mid-values of blowing ratio. The effect of the angle of the hole injection was performed by Yepuri et al. [13]. They found an improvement in the heat transfer and cooling effectiveness with the increase in the hole injection angle. Also, the effects of various injection hole shapes on film cooling performance were performed by Teng et al. [14], Yang et al. [15], and Abdelghany et al. [16].

The effect of blade rotation speed was examined in [17-19]. Rezasoltani et al. [17] mentioned that as the rotation speed increases from 2400 to 3000 rpm film cooling effectiveness also increases. Li et al. [4] found that the film cooling effectiveness enhances as the rotation speed increases from 400 to 700 rpm. Zhang et al. [18] found that film cooling effectiveness reduces with the increase of rotation speed, while Tao et al. [19] found that as the rotational speed rises the effectiveness is firstly improved and then worsened.

The present study aims to numerically investigate the film cooling effectiveness under different conditions from blowing ratios, Reynolds numbers, and especially rotation speeds in the range of 0 - 4600 rpm to clarify the difference in [17-19].

II. NUMERICAL METHOD

A. Theory and calculation

The Reynolds number (Re) of the hot mainstream is evaluated based on the length of the blade chord (C), hot mainstream density (ρ_∞), mainstream inlet velocity (U_∞), and mainstream dynamic viscosity (μ_∞) as follows:

$$\mathbf{Re} = \frac{\rho_\infty U_\infty C}{\mu_\infty} \qquad (1)$$

The blowing ratio (M) is an important parameter which affecting the blade surface's film cooling protection and is defined as [1]:

$$\mathbf{M} = \frac{\rho_\mathrm{c} U_\mathrm{c}}{\rho_\infty U_\infty} \qquad (2)$$

where ρ_c is the density of the coolant and U_c is the coolant inlet velocity the film hole.

The averaged film cooling effectiveness (η_{av}) is defined as [1]:

$$\boldsymbol{\eta_{av}} = \frac{T_\infty - T_\mathrm{w}}{T_\infty - T_\mathrm{c}} \qquad (3)$$

where T_c is the temperature of the coolant, T_∞ is the mainstream temperature, and T_w is the average wall temperature.

B. Physical model

A gas turbine blade with a 300 mm chord length (C), 170 mm axial chord length (Cx), and a blade height of 62 mm was used. As shown in Fig. 1, the angle (α) between the blade chord and the cascade inlet plane was set as 35.7° and the primary flow angle (β) was set as 90° [11]. For the arrangement of the film holes row, three positions on the blade surface were used; from the leading edge at 10%, 31%, and 69% of the axial chord length as shown in Fig. 1. One row of eleven cylindrical holes was set at the suction side of the blade as shown in Fig. 2. Each hole has a diameter of 2 mm (d), the distance from hole to hole center was set as 5 mm (2.5d) [3] and [11]. The film hole geometry is best described in Fig. 3. At the center of the exit of the injection hole, coordinate origin is set. The x-direction along the arc line of the suction wall was defined in the streamwise direction and the y-direction was defined normally to the suction wall.

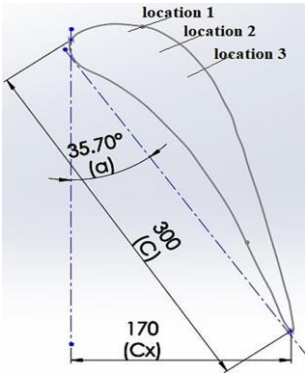

Fig. 1. Schematic diagram of test blade.

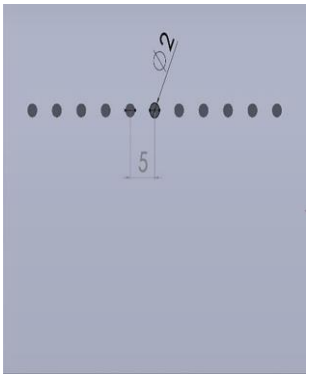

Fig. 2. One row of eleven holes.

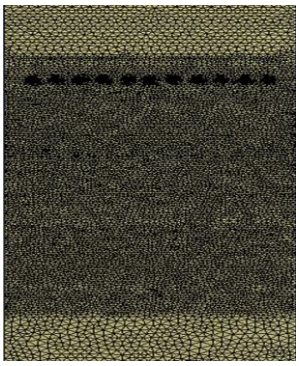

a) Mesh around coolant holes on the blade top view.

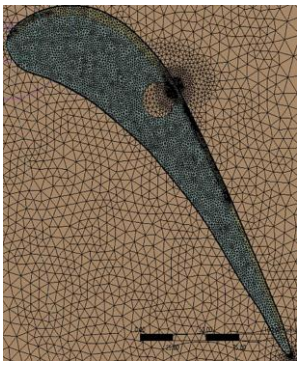

b) Mesh of solid blade and fluid domain.

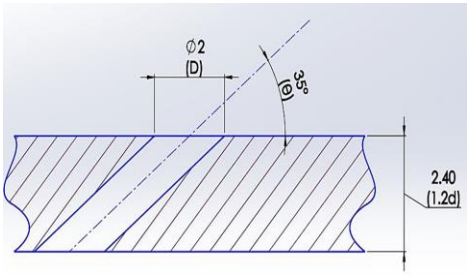

Fig. 3. Cylindrical hole cross section.

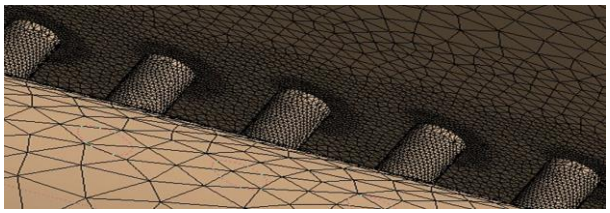

c) Section in coolant fluid domain mesh.

Fig. 4. Schematic diagram of computational model mesh.

C. *Grid properties*

Numerical simulation performance is closely connected to the model of turbulence and the mesh setup. ANSYS mesh, as shown in Fig. 4, was used for creating an unstructured non-conformal mesh with 4.2 million computational elements. At all locations with a growth rate of 1.2, all solid walls with a wall neighboring-cell y^+ value below 2.5 were applied. After a series of grid sensitivity checks, the final mesh was taken before the results were independent of the mesh. By using Fluent-CFD software, a three-dimensional simulation was done and a realizable k-ε was used as the turbulence model. Convergence was achieved.

D. *Boundary conditions*

Based on the periodicity of the flow, a single cascade blade was selected as the computational domain as shown in Fig. 5. Three subzones: plenum coolant flow zone, mainstream hot flow zone, and injection film holes coolant flow zones make up the fluid domain. The constant inlet velocity was taken at the mainstream inlet with constant values ranged from 2.4 m/s to 34 m/s. Mainstream length scale of 0.04 m and turbulence intensity of 2% were used. Zero gage pressure was set at the outlet flow boundary condition as the outlet pressure. All blade solid walls were treated as a solid-liquid interface. The constant inlet velocity was taken at the coolant plenum inlet with constant values ranged from 0.3 m/s to 5.2 m/s, coolant length scale and turbulence intensity, were 0.024 m and 2%, respectively. The hot stream inlet and coolant inlet temperatures were taken as 1500 K and 650 K, respectively. The blowing ratios, Reynolds numbers, and rotation speeds used in the investigation are listed in Table 1.

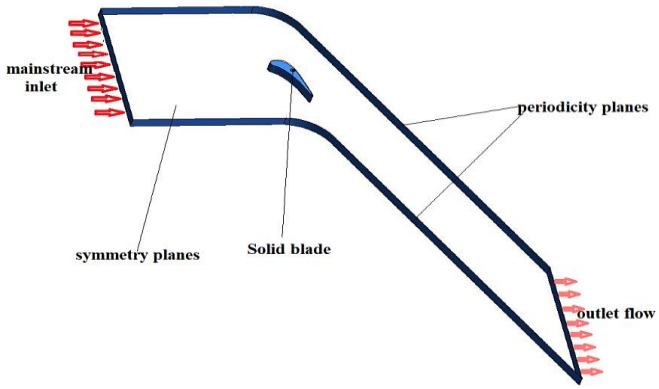

Fig. 5. Schematic diagram of computational domain.

TABLE 1.
BLOWING RATIOS, REYNOLDS NUMBERS, AND ROTATIONAL SPEEDS CASES.

Blowing ratio (M)	Reynolds number (Re)		Rotation speed (R)	
M1 = 0.91	Re 1	Re = 50,000	R1	200 rpm
M2 = 1.2	Re 2	Re = 87,000	R2	700 rpm
M3 = 1.5	Re 3	Re = 300,000	R3	900 rpm
M4 = 1.8	Re 4	Re = 500,000	R4	1600 rpm
M5 = 2	Re 5	Re = 700,000	R5	2400 rpm
			R6	3000 rpm
			R7	3600 rpm
			R8	4000 rpm
			R9	4600 rpm

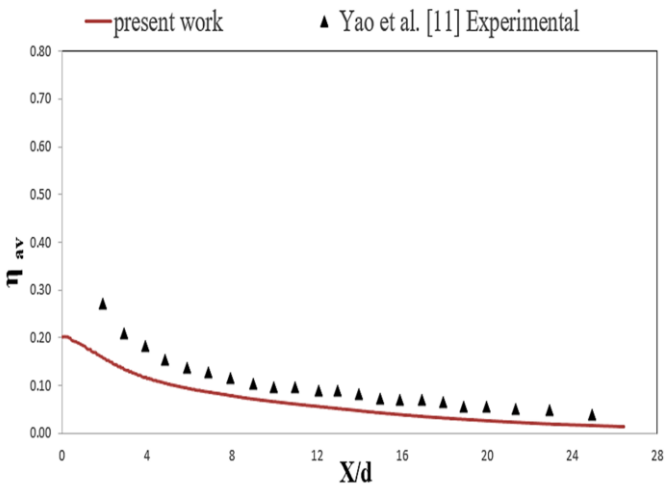

Fig. 6. Validation of present numerical work with experimental one.

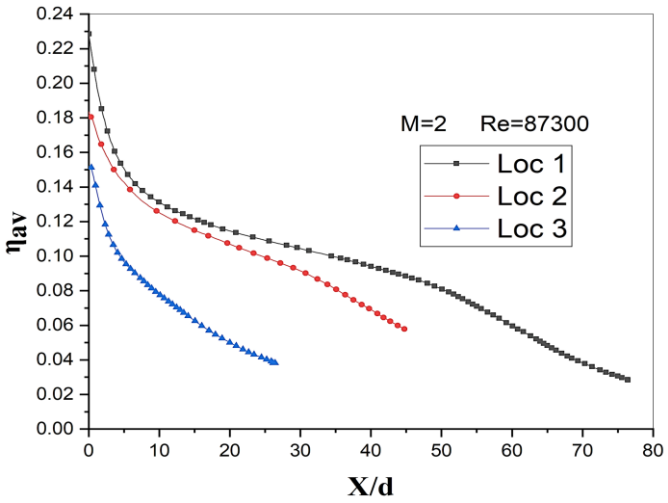

Fig. 7. Distribution of film cooling effectiveness without rotation at Re=87,300 at the three different film holes row locations.

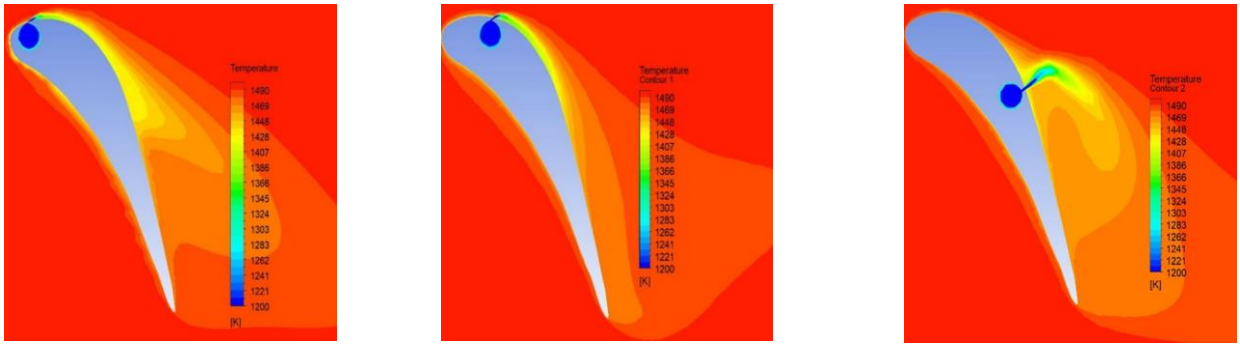

Location 1 & R=0 rpm Location 2 & R=0 rpm Location 3 & R=0 rpm

Fig. 8. Temperature contours at midplane for the three locations cases, Re=87,300 and M=2.

E. Model validation

The present simulation results are validated with the experimental results of Yao et al. [11]. The numerical simulation is performed at Reynolds number (Re) = 87,300, blowing ratio (M) = 0.91, and the inlet hot stream and inlet coolant temperatures are 333 K and 298 K, respectively. A good agreement between the present simulation results and the experimental ones is noticeable as shown in Fig. 6.

III. RESULTS AND DISCUSSION

A. Effect of the film holes row location

Three locations on the blade surface were used for the arrangement of the row of film holes; from the leading edge at 10%, 31%, and 69% of the axial chord length. Fig. 7 shows the average film cooling effectiveness variation all over the blade surface at M=2 and Re=87,300 at the three locations. It is noticed that for stationary cases, location 1 indicates the highest film cooling effectiveness. Near the film holes, the enhancement in film cooling effectiveness of location 1 is by 22% than location 2 and 35% than location 3 as shown in Fig.7.

The blade film coverage area is best described by temperature contours. Fig. 8 shows the temperature contours at the blade midplane (x-y plane) for the three locations without blade rotation at M=2 and Re=87,300. Location 1 shows better film coverage area than others.

B. Effect of blowing ratio (M)

Fig. 9 shows the variation of the averaged film cooling effectiveness downstream of the film hole jets at the blade midplane (x-y plane) of location 1 for five blowing ratios 0.91, 1.2, 1.5, 1.8, and 2 without blade rotation. For location 1, the effectiveness is enhanced by 57% as the blowing ratio increases from M=0.91 to M=2. Film cooling effectiveness has optimum value near the film hole outlet. As the film coolant spread away from the film hole outlet, the opportunity of the hot stream and coolant mixing increases, which worsens the film cooling effectiveness along the blade stream-wise directions. Fig. 10 shows the temperature contours at the blade midplane (x-y plane) for five blowing ratios without blade rotation. It's found that film coverage increases as the blowing ratio increases.

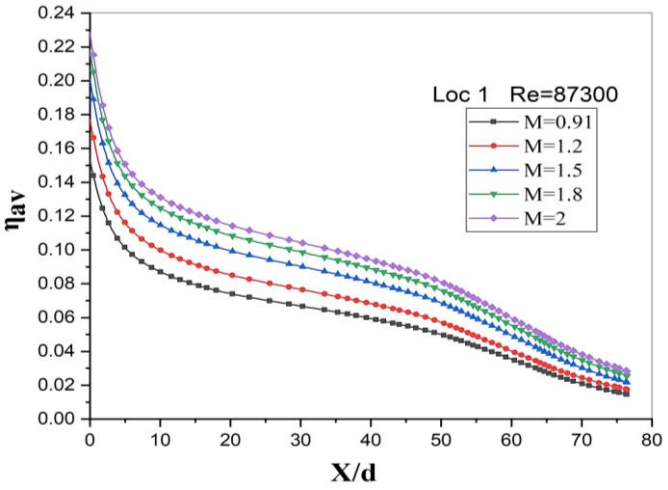

Fig. 9. Distribution of film cooling effectiveness without rotation at Re=87,300.

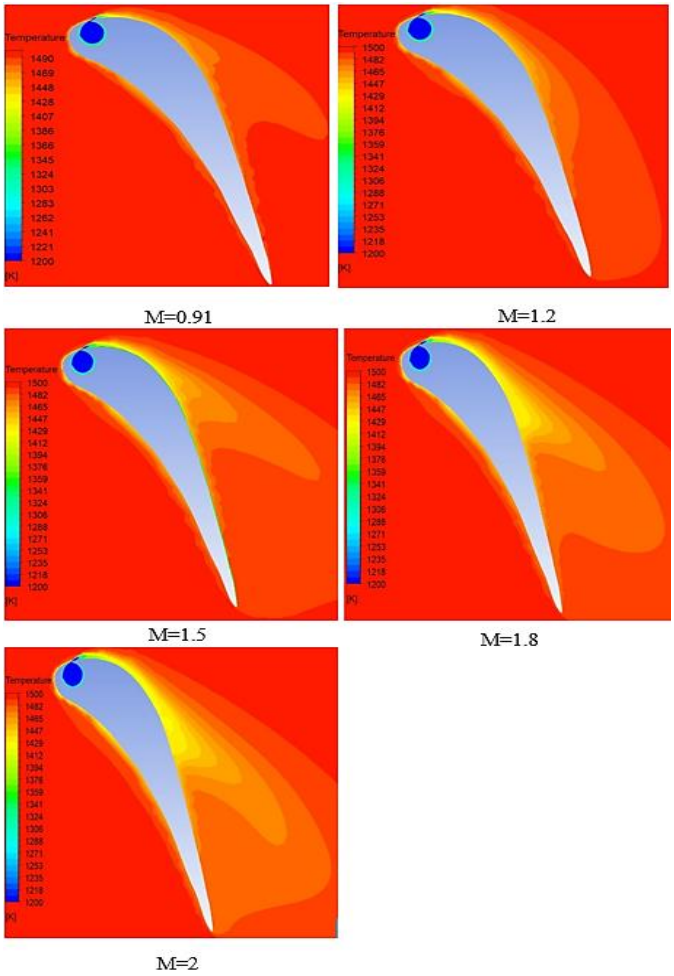

Fig. 10. Temperature contours at midplane at different blowing ratios, Re=87,300, and R=0 rpm at location 1.

C. *Effect of rotation* (*R*)

The film cooling effectiveness variation at M=2 and Re=87,300 with the rotational speed from 0 to 4600 rpm is depicted in Fig. 11a. It shows the film cooling effectiveness variation at specific locations in the blade, whereas the variation all over the blade in the streamwise direction is shown in Fig. 11b. The film cooling effectiveness increases slightly from 0 rpm until it reaches the highest value at 900 rpm then decreases with the increase in rotation speed. Also, the lowest value of film cooling effectiveness is for the stationary cases as shown in Fig. 11a and Fig. 11b.

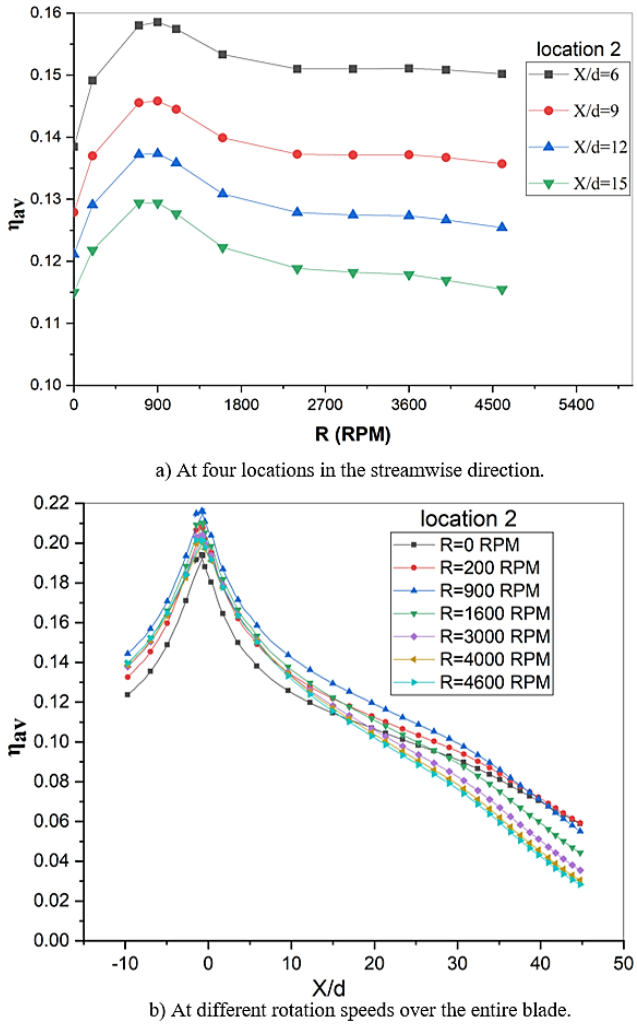

Fig. 11. Distribution of film cooling effectiveness at M=2 and Re=87,300 for location 2.

Fig. 12 shows the temperature contours at the midplane (x-y) for M=2 at different rotation speeds and Re=87,300. It is found that the largest film coverage area was for R= 900 rpm and it decreases slightly as rotation speed increases, which explains the decrease in film cooling effectiveness when the rotation speed increases more than 900 rpm

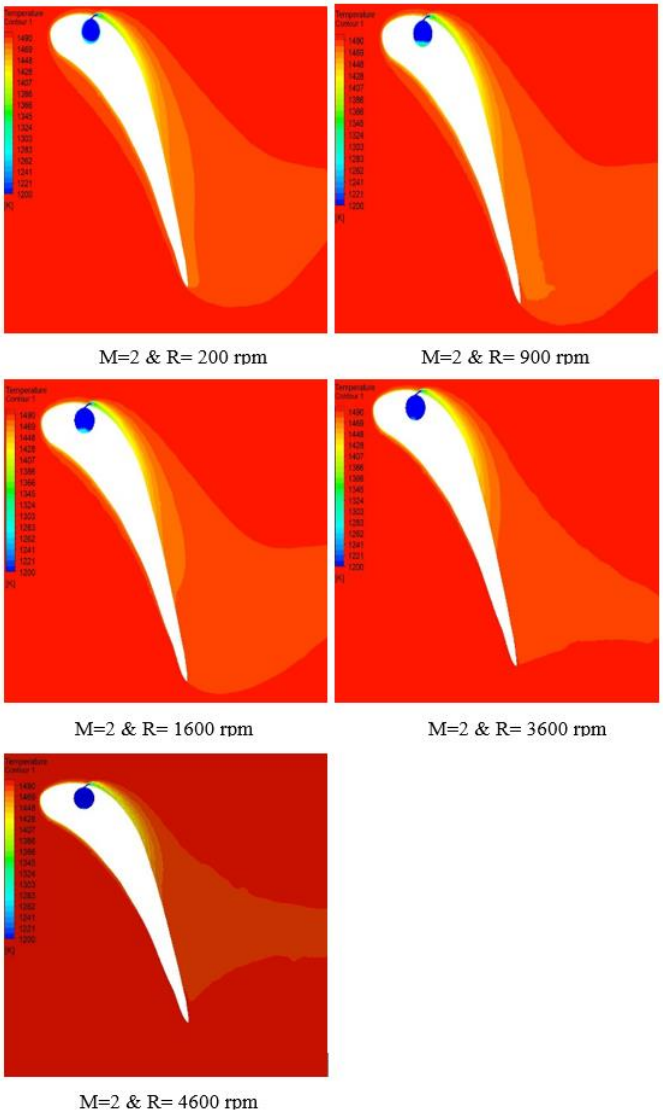

Fig. 12. Temperature contours at midplane (x-y) for M=2 at different rotation speeds at Re=87,300 for location 2.

D. *Effect of Reynolds number* (Re)

Five different Reynolds numbers of 50,000, 87,300, 300,000, 500,000, and 700,000 have been used to study the effect of Re on film cooling effectiveness at constant inlet coolant hole velocity U_c, hole=8.5 m/s, and 3000 rpm for location 3 as shown in Fig. 13. It is found that as the Reynolds number increases, the film cooling effectiveness reduces because of the increase in the hot mainstream momentum. Fig. 14 shows the temperature contours at the blade midplane (x-y plane) for the five Reynolds numbers at constant velocity and rotation speed = 3000 rpm. It's found that the best film coverage area was for Re=50,000 and the coverage area reduces as the Reynolds number increases.

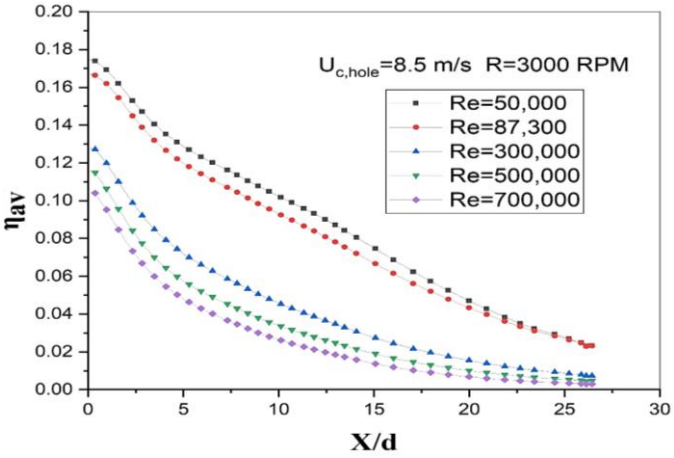

Fig. 13. Distribution of film cooling effectiveness with different Reynolds numbers at constant velocity at location 3.

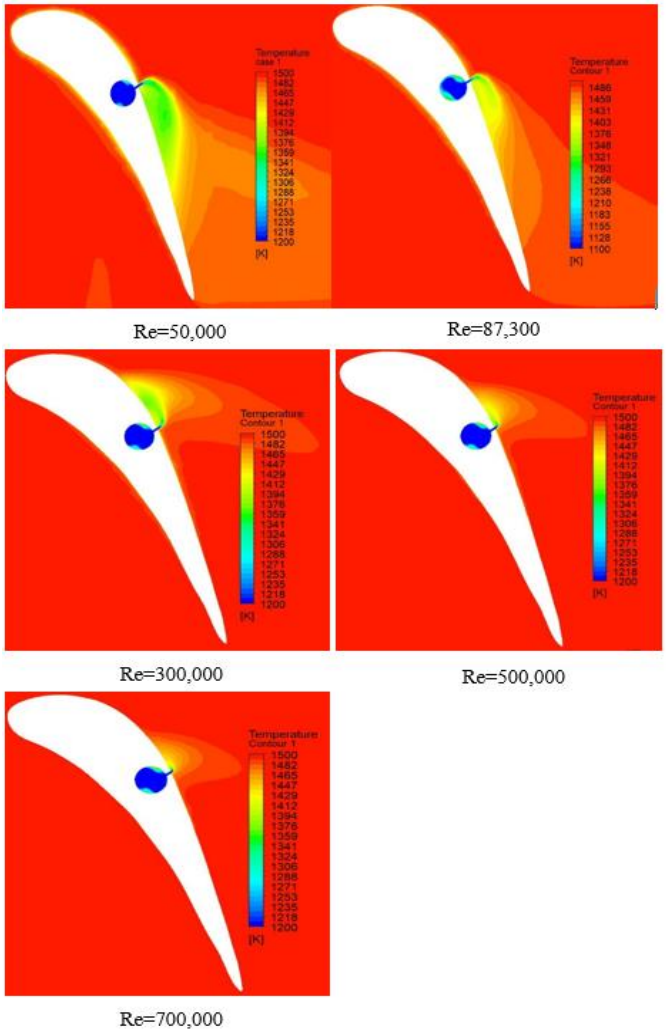

Fig. 14. Temperature contours at blade surface at midplane (x-y) for the five Reynolds numbers at U_c = 8.5 m/s and R=3000 rpm at location 3.

Fig. 15 shows the flow velocity magnitudes over the blade at midplane (x-y) for R=3000 rpm, M=2, and the five Reynolds numbers. It is noticed that as the Reynolds number

increases, eddies size increases which increases the fluid mixing and forming a bad film coverage area on the blade. Also, as the Reynolds number increases from Re= 300,000 to 700,000, the coolant jet direction was reversed due to the increase in the eddies size which draws the coolant jet in the reversed direction.

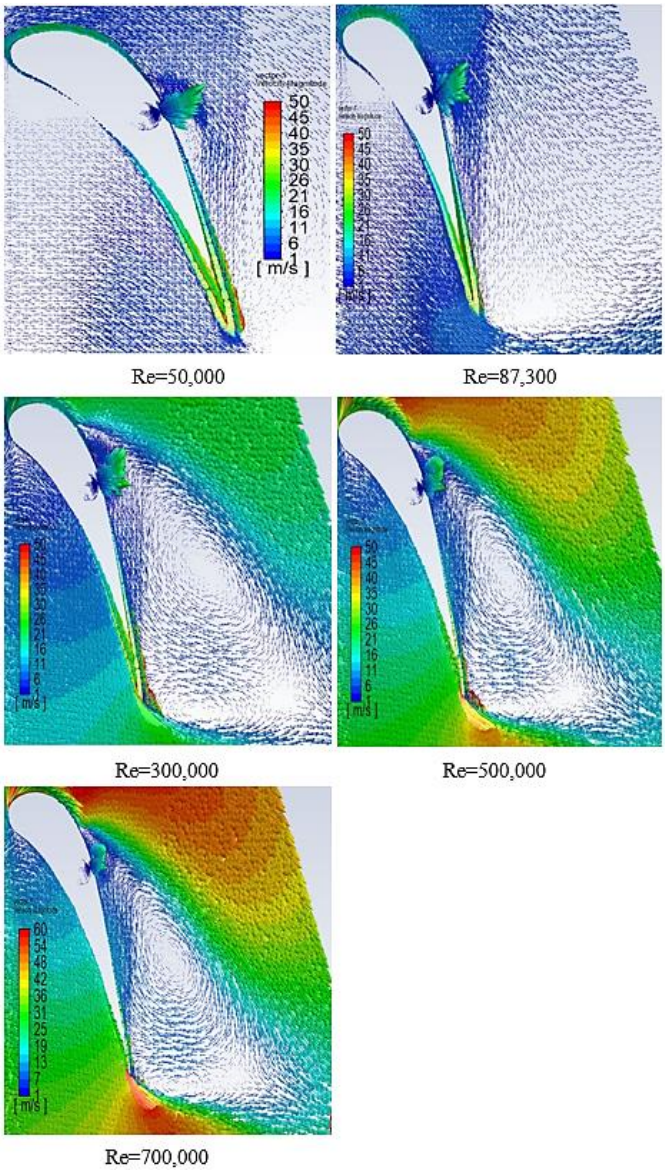

Fig. 15. Flow velocity magnitude over the blade at midplane (x-y) for U_c = 8.5 m/s at R=3000 rpm and the five Reynolds numbers at location 3.

IV. Conclusion

The turbine blade suction side film cooling with a single row of eleven cylindrical holes has been investigated numerically using the realizable k-ε as the turbulence model. The effects of film holes row location, blowing ratio, rotation speed, and Reynolds number are studied at three locations on the blade surface, five blowing ratios, five Reynolds numbers, and nine rotation speeds. The results are summarized as follows:

1. Location 1 indicates the highest average film cooling effectiveness and best film coverage area.
2. The average film cooling effectiveness enhances as the blowing ratio increases and has the largest value near the film hole exit.
3. Along the blade, as the surface temperature increases, the film cooling effectiveness reduces.
4. The film cooling effectiveness rises as the rotational speed increases from 0 rpm until it reaches its optimum value at 900 rpm.
5. As the Reynolds number rises, the film cooling effectiveness reduces.
6. The best film coverage area on the blade surface was for Re=50,000.

References

[1] A. F. El-Sayed, Aircraft Propulsion and Gas Turbine Engines, 2nd Edition, Taylor & Francis, 2017, p. 1447.
[2] H. Saravanamuttoo, G. F. C. Rogers, H. Cohen, P. V. Straznicky, and A. C. Nix, Gas Turbine Theory, 7th Edition, 2017, p. 606.
[3] J. C. Han, S. Dutta, and S. Ekkad, Gas Turbine Heat Transfer and Cooling Technology, 2nd Edition, Taylor & Francis Group, New York, 2013, p. 843.
[4] H. Li, F. Han, H. Wang, Z. Zhou, and Z. Tao, "Film cooling characteristics on the leading edge of a rotating turbine blade with various mainstream Reynolds numbers and coolant densities," International Journal of Heat and Mass Transfer, Vol. 127, (2018), pp. 833–846.
[5] S. B. Islami and B. A. Jubran, "The effect of turbulence intensity on film cooling of gas turbine blade from trenched shaped holes," Heat and Mass Transfer, Vol. 48, No. 5, (2012), pp. 831–840.
[6] V. P. Lebedev, V. V. Lemanov, S. Y. Misyura, and V. I. Terekhov, "Effects of turbulence on film coding efficiency," International Journal of Heat and Mass Transfer, Vol. 38, No. 11, (1995), pp. 2117–2125.
[7] S. Mhetras and J. C. Han, "Effect of Unsteady Wake on Full Coverage Film-Cooling Effectiveness for a Gas Turbine Blade," 9th AIAA/ASME Joint Thermophysics and Heat Transfer Conference, 5 - 8 June 2006, San Francisco, California, pp. 1–17.
[8] J. S. Kwak and J. C. Han, "Heat transfer coefficients and film-cooling effectiveness on a gas turbine blade tip," Journal of Heat Transfer, Vol. 125, June 2003, pp. 494–502.
[9] V. K. Garg and R. E. Gaugler, "Effect of coolant temperature and mass flow on film cooling of turbine blades," International Journal of Heat and Mass Transfer, Vol. 40, No. 2, (1997), pp. 435–445.
[10] C. Liu, H. Zhu, J. Bai, and D. Xu, "Film cooling performance of converging slot-hole rows on a gas turbine blade," International Journal of Heat and Mass Transfer, Vol. 53, (2010), pp. 5232–5241.
[11] Y. Yao, J. Z. Zhang, and L. P. Wang, "Film cooling on a gas turbine blade suction side with converging slot-hole," International Journal of Thermal Sciences, Vol. 65, (2013), pp. 267–279.
[12] C. Q. Nguyen, P. L. Johnson, B. C. Bernier, S. H. Ho, and J. S. Kapat, "Comparison of Film Effectiveness and Cooling Uniformity of Conical and Cylindrical-Shaped Film Hole with Coolant-Exit Temperature Correction," ASME Turbo Expo 2010: Power for Land, Sea, and Air, Paper GT2010-23732, pp. 1–11.
[13] G. B. Yepuri, G. Lalgi, A. Puttarangasetty, F. Jesuraj, S. Kenkere, and V. Nanjundaiah, "Experimental and Numerical Investigation of Effect of Blowing Ratio on Film Cooling Effectiveness and Heat Transfer Coefficient over a Gas Turbine Blade Leading Edge Film Cooling Configurations," Proceedings of the ASME 2013 Gas Turbine India Conference GTINDIA2013, Paper GTINDIA2013-3552, pp. 1–10.
[14] S. Teng, J. C. Han, and P. E. Poinsatte, "Effect of film-hole shape on turbine-blade film-cooling performance," Journal of Thermophysics and Heat Transfer, Vol. 15, No. 3, July September 2001, pp. 257–265.
[15] H. Yang, H. C. Chen and J. C. Han, "Film-cooling prediction on turbine blade tip with various film hole configurations," Journal of

Thermophysics and Heat Transfer, Vol. 20, No. 3, July–September 2006, pp. 558–568.

[16] E. S. Abdelghany, A. F. El-Sayed, M. A. Fouad, and E. E. Khalil, "Effect of Shaped-Hole on Film Cooling Effectiveness of Gas Turbine Blade," 10th International Energy Conversion Engineering Conference, 30 July - 01 August 2012, Atlanta, Georgia, AIAA 2012-3986, pp. 1–17.

[17] M. Rezasoltani, M. T. Schobeiri, and J. C. Han, "Experimental investigation of the effect of purge flow on film cooling effectiveness on a rotating turbine with nonaxisymmetric end wall contouring," Journal of Turbomachinery, Vol. 136, No. 9, 091009, (2014), pp. 1–10.

[18] D. H. Zhang, M. Zeng, and Q. W. Wang, "The Influence of Rotating Speeds on Film Cooling Characteristics on GE-E3 Blade Tip with Different Tip Configurations," ASME Turbo Expo 2009: Power for Land, Sea, and Air, Paper GT2009-60295, pp. 1–9.

[19] Z. Tao, X. Yang, S. Ding, G. Xu, H. Wu, H. Deng, X. Luo, "Experimental study of rotation effect on film cooling over the flat wall with a single hole," Experimental Thermal and Fluid Science, Vol. 32, No. 5, (2008), pp. 1081–1089.

Title Arabic:

التحقيق في فعالية التبريد الغشائي تحت ظروف مختلفة من أرقام رينولدز وسرعة الدوران

Arabic Abstract:

تم دراسة فعالية تبريد الغشاء لجانب ريشة التوربين تحت أرقام رينولدز المختلفة وظروف الدوران عدديًا. تم فحص ثلاثة مواقع لصف ثقوب مانع التبريد وهي على مسافة من الحافة الأمامية للشفرة عند ١٠% و ٣١% و ٦٩% من طول الوتر المحوري. يتم حقن سائل التبريد من أحد عشر ثقبًا أسطوانيًا بسرعات دوران تتراوح من ٠ إلى ٤٦٠٠ دورة في الدقيقة وتراوحت نسب النفخ من ٠.٩١ إلى ٢. يتم إجراء الفحص في خمسة أرقام رينولد للغازات الساخنة وهي ٥٠٠٠٠ و ٨٧٣٠٠ و ٣٠٠٠٠٠ و ٥٠٠٠٠٠ و ٧٠٠٠٠٠. درجة حرارة مدخل سائل التبريد هي ٦٥٠ كلفن بينما درجة حرارة دخول الغازات الساخنة هي ١٥٠٠ كلفن لجميع الحالات. يُظهر الموقع ١ أعلى فعالية لتبريد الريشة. الزيادة في فعالية تبريد الغشاء للموقع ١ عن الموقع ٢ هي بنسبة ٢٢% وعن الموقع ٣ بنسبة ٣٥%. بالنسبة للموقع ١ يُنظر مباشرة إلى زيادة بنسبة ٥٧% في فعالية تبريد الغشاء عن الموقع ٢ وذلك مع زيادة نسبة النفخ من ٠.٩١ إلى ٢. بالنسبة للموقع ٢ تزداد فعالية تبريد الغشاء مع زيادة سرعة الدوران من ٠ دورة في الدقيقة حتى تصل إلى القيمة المثلى لها عند ٩٠٠ دورة في الدقيقة. كما أظهرت النتائج أن فعالية تبريد الغشاء تقل مع زيادة رقم رينولدز نتيجة زيادة كمية الحركة للمائع الساخن.